Carbohydrate Polymers 186 (2018) 394–401

Contents lists available at ScienceDirect

Carbohydrate Polymers

journal homepage: www.elsevier.com/locate/carbpol

Extraction and characterization of polysaccharides from tamarind seeds, rice mill residue, okra waste and sugarcane bagasse for its Bio-thermoplastic properties

C. Chandra Mohan[a], K. Harini[a], B. Vajiha Aafrin[a], U. Lalitha priya[a], P. Maria jenita[a], S. Babuskin[b], S. Karthikeyan[a], K. Sudarshan[a], V. Renuka[a], M. Sukumar[a,*]

[a] Centre for Food Technology, Anna University, Sardar Patel Road, Guindy, Chennai, 600025 Tamilnadu, India
[b] Department of Industrial chemistry, Abaya campus, Arba Minch University, Ethiopia

ARTICLE INFO

Keywords:
Tamarind seed (urigam)
Okra mucilage
Sugarcane bagasse cellulose
Residual rice bran starch
Bio-thermoplastics
Thermal stability

ABSTRACT

The aim of the present study is to extract potential thermoplastic polysaccharides from agricultural industrial wastes. Polysaccharides were extracted from renewable agro industrial wastes such as tamarind seeds [rich in starch (TSS)], okra head waste [rich in mucilage polysaccharide (OMP)], sugarcane bagasse [rich in cellulose (SBC)] and residual rice mill wastes [rich in starch and fiber (RS)]. Urigam variety of tamarind seed starch found to be an amylose rich starch. Different polysaccharides extracted from agro wastes were found to be having high thermal stability, except okra polysaccharide (comparatively low). X-ray diffraction pattern of tamarind seed starch proved its high crystallinity index. Crystallinity index of investigated polysaccharides were found to be in the order of SBC > TSS > RS > OMP. Chemical nature of extracted polysaccharides was confirmed by Fourier transform infrared spectroscopic analysis. Residual rice bran starch granules and tamarind seed starch globules were found to be having comparatively reduced particle size than sugarcane bagasse cellulose and okra mucilage. Scanning electron microscopic analysis revealed the cluster formations of RS granules and TSS globules. Residual rice bran starch found to be associated with other fibers (present in outer coat of rice). Okra mucilage and SBC were examined to be having linear sheets and linear bundles structures, respectively.

1. Introduction

Petrochemical based plastics are well established for its use in all packaging industries, but these petrochemical plastics raise serious environmental issues, as they are not easily biodegradable. As a result, accumulation of petrochemical plastics has become the biggest concern to the society (Yuliana, Huynh, Hob, Truong, & Ju, 2012). Many researchers have worked on development of alternative source of polymer materials. Natural polymers such as polysaccharides provide the remedy for this serious environmental concern, as they are naturally disintegrated by microbe present in environment. Carbohydrates (Sudharsan et al., 2016; Yuliana et al., 2012), proteins (Wang, Sun, & Huang, 2010) and fibers (Imam et al., 2008) are some of the natural polymers which are currently under study for development of bioplastics.

Agricultural waste materials are renewable in nature, since they are coming out in large amount from agro-food processing industries. These wastes are also a rich source of natural polysaccharide materials, thus they provide good alternative for petrochemicals with cheap economic values (Sudharsan et al., 2016; Yuliana et al., 2012). Raw material processing food industries produce lot of agricultural wastes. Sugar industries produce sugarcane bagasse as waste, are found to be rich in cellulose (Candido & Gonclave, 2016). These cellulose are high molecular weight homopolysaccharide composed of β-1, 4-anhydro-D-glucopyranose units [$C_{6n}H_{10n}O_2$ (5n + 1) (n = degree of polymerization of glucose)] and is considered to be the most abundant polymer in nature (Gutierrez & Alvarez, 2017). Rice milling industries produce residual Rice Bran waste (coming out of milling process); these rice bran wastes are rich in starch, fiber and associated proteins. Generally starch has a granular structure and is composed of two macromolecules: amylose and amylopectin. Amylose is a linear polymer formed by glucose units linked by α - (1, 4) whereas amylopectin is a highly branched polymer of glucose units with ramifications in α - (1, 6) (Cano, Jimenez, Chafer, Gonzalez, & Chiralt, 2014). Tamarind seeds are coming out as waste in large quantity from tamarind pulp industries; these seeds found to be are rich in Xyloglycan starch (Sudharsan et al., 2016). These starch

* Corresponding author.
E-mail address: sukumar@annauniv.edu (M. Sukumar).

https://doi.org/10.1016/j.carbpol.2018.01.057
Received 11 December 2017; Received in revised form 16 January 2018; Accepted 17 January 2018
Available online 31 January 2018
0144-8617/

molecules composed of (1–4)-β-D-glucan backbone substituted with side chains of α-D-xylopyranose and β-D-galactopyranosyl (1,2)- α-D-xylopyranose linked (1–6) to glucose residues. The glucose, xylose and galactose units are present in the ratio of 2.8:2.25:1.0 (Goyal, Kumar, & Sharma, 2007). Okra head portions are cut down and thrown out as waste in okra processing industries. Mucilage of okra found to contain polysaccharide with repeating units of α - (1,2)-rhamnose and α - (1–4) -galacturonic acid residues with disaccharide side chains with degree of acetylation (DA = 58) (Sengkhamparn, Verhoef, Schols, & Sajjaanantakul, 2008).

This main aim of this study, focus on extraction and isolation of polysaccharide materials from four different agricultural wastes (Sugarcane bagasse, Tamarind seeds, Okra head waste and Rice bran wastes), for its potential biopolymer properties. Isolated polysaccharide materials were characterized through different instrumental analytical methods, to examine its Proximate, Thermal, Particle and Structural properties. Moreover it is also the aim of the subsequent study (Chandra mohan et al., 2016), to examine the rheological properties of investigated polysaccharides in combinations and to investigate their effect on starch based Bio-thermoplastic film properties produced at different film casting conditions (Hot air oven, Microwave oven & Ultraviolet irradiation method).

2. Materials and methods

2.1. Raw materials

Tamarind seeds (variety: Urigam) [having moisture content of 4.58 ± 1.52% (w/w)] were collected from Dharmapuri district, Tamilnadu, India. Residual rice bran powder [having moisture content of 10.32 ± 2.43% (w/w)], was collected from local rice mills in Chennai, Tamilnadu, India and waste sugarcane bagasse [having moisture content of 16.57 ± 4.26% (w/w)], was collected from sugar factories in and around Chennai, Tamilnadu, India. Okra head waste [having moisture content of 14.25 ± 3.22% (w/w)] was collected from nearby okra processing industries in and around Chennai, Tamilnadu, India. All the chemicals and solvents were procured from Merck (Germany) Purity-EMPARTA^{ACS}.

2.2. Extraction of polysaccharides

2.2.1. Tamarind seed starch (T)

Tamarind seed starch was extracted using the method described in our previous study (Sudharsan et al., 2016), with slight modification at alkaline wash of starch. Tamarind seeds are roasted and decorticated. Seeds are then broken into smaller pieces in a Philips HI1645 750W grinder (Koninklijke Philips N.V., Amsterdam, Netherland) pulverized to make starch powder. Pulverized TSS powder was defatted using methanol at 65 °C and *n*-hexane at 69 °C for 10 h each, in a Soxhlet extractor. Defatted starch was washed with 70% ethanol and 0.1 M NaOH for 5 min in each solvent (5 times) and centrifuged at 10,000*g* for 15 min, to remove protein molecules associated with starch. The starch powder thus obtained is mixed with water and re-filtered twice using 200 mesh screens and then washed successively with 0.1 M NaOH (3 times) and deionized water. Finally, starch powder was dried in an oven at a temperature of 50 °C till it reaches constant weight. Thus prepared starch was packed in polythene bags and stored at −5 °C for further studies.

2.2.2. Residual rice bran starch (R)

The rice processing residual waste (bran) were subjected to ground in a Haystar flour mill (Haystar, Maharashtra, India) and then sieved in 100 mesh sieve to obtain rice starch powder. This RS powder was subjected to alkaline extraction method described by Dhital, Butardo, Jobling, and Gidley (2015). Extracted RS powders were dried at 50 °C in hot air oven till it reaches constant weight. Dried RS powders were stored in polythene bags at −5 °C, for further studies.

2.2.3. Okra polysaccharides (OK)

Okra mucilage polysaccharide was extracted using the method described by Alamri et al. (2017). Okra head waste was dried in fluidized bed drier (Tronado, Armfield) at 40 °C, till it reaches constant weight. Dried okra head portions were powdered and blended with 0.05 M NaOH for 5 min. Blended samples were centrifuged at 2000*g*, the supernatant was collected and the extraction procedure was repeated on pellet sample. Supernatants were combined and adjusted to pH of 7 and freeze dried to store at −5 °C, in polythene bags.

2.2.4. Sugarcane bagasse cellulose (C)

Sugarcane bagasse cellulose was extracted using the method described by Kasa et al. (2017). Pre-treatment was conducted in order to remove lignin and hemicellulose in banana stem fibers. Sugarcane bagasse's were washed in distilled water three times to remove residual sugars. Washed sugarcane bagasse's were dried in hot air oven and powdered. Sugarcane bagasse powder was subjected to lignin and hemicellulose removal by blending with 2% of NaOH solution at 80 °C for 4 h. Then the blended sugarcane bagasse powder was washed with deionized water and filtered through Watman filter paper No.41. Thus extracted cellulose was bleached with acetate buffer (27 g NaOH and 75 mL glacial acetic acid diluted to 1 L of distilled water) and sodium chlorate (1.7 wt% $NaClO_3$ in distilled water) mixture (1:1) at 300 rpm for 4 h. Thus obtained bleached SBC powder was filtered and neutralized to pH 7 followed by drying in Hot air oven at 40 °C till constant weight.

2.3. Characterization of polysaccharides

2.3.1. Proximate analysis

The total starch content was determined by the method previous described by Association of Official Analytical Chemists (AOAC) (1996). The nitrogen content of samples was assessed by Kjeldahl method to estimate the crude protein content of samples (AOCS Official Method Ba 4a-38, 1997) and ash content was estimated by method described in AOCS Official Method Ba 5a-49 (1997). Total moisture content present in the sample was determined by the method previously described by AOAC (1996). Crude fiber of polysaccharides was analyzed by using the modified method of Prosky, Asp, Scheweizer, de Vries, & Furda, 1988. Cellulose content of SBC powder was estimated through the method described by Updegraff, 1969. Amylose content of TSS and RS was estimated using the method described by Sadasivam and Manickam (1996). Total amylose content was analyzed using an Evolution 201 UV–vis spectrophotometer (Thermo Fisher Scientific, USA) at 590 nm.

2.3.2. TG-DSC analysis

TG-DSC analyses were performed in NETZSCH STA 449F3 (NETZSCH-Gerätebau GmbH, Germany) instrument. 10 ± 3 mg of the sample was placed in alumina pan (AL 203) and heated at a rate of 10 °C/min from ambient temperature until it reached 1400 °C in a nitrogen atmosphere with flow rate of 20 mL/min, to avoid unwanted by-product production in presence of oxygen. Empty alumina pan was used as reference (Sudharsan et al., 2016).

2.3.3. X-ray diffraction analysis

Wide angle X-ray diffraction measurements were carried out using D8 Advance X-ray powder diffractometer (Bruker, USA) equipped with one-dimensional Debye–Scherr camera, Cu Ka radiation (wavelength 0.1542 nm) operates at 40 kV and 35 mA. The crystallinity index (CI) was calculated using Eq. (1), by measuring the peak height of the crystalline region (I_{cry}) and the amorphous region (I_{am}). (Sudharsan et al., 2016; Dos Santos, Leonel, Garcia, do Carmo, & Franco, 2016)

$$CI\,(\%) = \frac{I_{cry}}{I_{total}} \times 100\% \quad (1)$$

Where I_{total} – Total area under XRD peaks [$I_{total} = I_{cry} + I_{am}$]

2.3.4. FTIR analysis

Fourier transform infrared spectroscopy (FTIR) was used to determine the chemical bonds, chemical nature and functional groups of extracted polysaccharides. The FTIR analysis was performed using Carry 660 (Agilent technologies, USA) FTIR. The dried active fraction of extracted polysaccharides (0.3–0.5 mg) were ground in about 80 mg of spectral grade KBr (sigma) and pressed into pellets under about 5–6 t cm^{-2} pressure with the help of a hydraulic press. The spectral measurements were carried out in an absorbance range of 400–4000 cm^{-1} with plain KBr pellet as the background reference (Sudharsan et al., 2016).

2.3.5. Particle size analysis

Particle size distribution of polysaccharides was measured in laser diffraction system (HELOS-BR, Sympatec Inc., Princeton, NJ, USA). Deionized water was used as the medium for wet size measurement of the polysaccharides. Sonic treatment was given to samples to avoid aggregation of particles (Sudharsan et al., 2016).

2.3.6. Scanning electron microscopic analysis

The surface micrographs of extracted polysaccharides were obtained through scanning electron microscope (HITACHI-S3400N, Japan). The extracted polysaccharides were scattered on the surface of a double-sided tape which is attached to a stub. The images were taken at an accelerating potential of 15 kV in different magnifications. Images were processed through Mountain Map Version 7 software (Digital surf, France), to measure the particle size of polysaccharides (Sudharsan et al., 2016).

3. Results and discussions

3.1. Extraction and characterization of polysaccharides

3.1.1. Proximate composition of polysaccharides

Tamarind seeds (urigam), okra head waste and sugarcane bagasse were dried in fluidized bed drier for 6–10 h at the temperature of 60 °C (Flow rate of 70 CFM). The dried samples were powdered and subjected to extraction procedures. Residual rice bran starch was brought as waste powder. Proximate composition of polysaccharides extracted from agro industrial wastes of tamarind seeds, okra waste, Residual rice bran starch and sugarcane bagasse cellulose was tabulated in Table 1. Tamarind seeds were found to have high amount of starch, it was also found to be rich in crude fiber and other minerals (ash). Okra waste was also found to have high amount of carbohydrate (okra polysaccharides is a type of carbohydrate thus it was detected in carbohydrate analysis). Similar observations are made by other researchers (Ghori et al., 2017). Okra mucilage was also found to be rich in associated proteins. This may be due to binding of protein molecules with okra polysaccharides (Alamri, Mohamed, Hussain, & Xu, 2017). Residual rice bran starch powder found to have high amount of rice starch and crude fiber, since the waste material from rice processing industries tends to have outer portions of rice grains. Sugarcane bagasse was examined to be rich in cellulose. Starch is classified into three groups based on amylose content, amylose-rich starch (amylose content > 30 wt.%), moderate amylose starch (amylose content 10–30 wt.%), and waxy starch (amylose content < 10 wt.%) (Lee, Lee, & Chung, 2017). Amylose content of tamarind seed starch and Residual rice bran starch were found to be 30.41 and 23.13%, respectively. Thus urigam variety tamarind seeds starch was found to be an amylose rich starch.

3.1.2. Thermal stability of polysaccharides

Thermal stability of polysaccharide samples extracted from different agricultural wastes was analyzed by Thermo gravimetric differential scanning calorimetric (TG-DSC) analysis. Fig. 1, depicts the thermal analysis results for all the extracted polysaccharides. Thermo Gravimetric Analysis (TGA), Derivative Thermo Gravimetric (DTG) and Differential Scanning Calorimetric (DSC) curves of tamarind seed starch are given in Fig. 1A. After initial dehydration weight loss (5.30%) of sample (Sudharsan et al., 2016), weight loss TGA curve of tamarind seed starch showed stable weight till 201.88 °C (93.10% weight). Major weight loss of 67.91% for tamarind seed starch occurred between 201.88 °C and 467.48 °C, which was confirmed by DTG with peak decomposition temperature of 322.01 °C. This major decomposition temperature of urigam variety tamarind seed starch was found to be lower than DTS – 1 variety tamarind seed starch (Sudharsan et al., 2016). The tamarind starch sample continued to decompose till it attains its residual mass of 15.18% at 1399.1 °C. TGA results of tamarind seed starch proved its thermal stability till 201.88 °C, thus any process for biopolymer film production from tamarind seed starch should be under this decomposition temperature. Differential scanning calorimetric curve of tamarind seed starch showed the energy requirement for the gelatinization and decomposition of the starch. Initial endothermic curve was noted at peak temperature of 90 °C with 128.32 mJ/mg energy requirement. Similar endothermic peak at ~90 °C was observed by Samal and Dangi, 2014. This gelatinization temperature depends on the glass transition of the starch. Two decomposition exothermic peaks were observed on 518.43 °C and 660.82 °C with energy release of 37.66 mJ/mg and 59.61 mJ/mg, respectively.

Fig. 1B, shows the TGA, DTG and DSC curves of Okra mucilage polysaccharide. Moisture loss or dehydration of sample was noted till 120 °C from 100% to 93.21% weight loss. According to derivative weight loss curve, major weight loss (44.87%) was noted between temperatures of 187.23 °C and 385.10 °C with onset peak weight loss temperatures of 271.68 °C and 325.08 °C. In these two weight losses, first weight loss may be due to phase transition and second weight loss may be due to decomposition (Prajapati, Jani, Moradiya, & Randeria, 2013). Beyond 385.10 °C, there was no major weight losses observed, but there was a constant weight loss due to decomposition of sample (Mishra & Sunita, 2007). The residual mass of okra polysaccharide was

Table 1
Proximate composition of extracted polysaccharides.

Components Units	Tamarind seed starch Dry weight [%, (w/w)]	Okra mucilage	Residual rice bran starch	Sugarcane bagasse cellulose
Moisture	1.08 ± 0.16	1.51 ± 0.32	0.98 ± 0.38	0.84 ± 0.26
Starch (Carbohydrate)	85.74 ± 0.75	80.32 ± 0.24	75.29 ± 0.43	N.D.
Cellulose	N.D.	1.59 ± 0.57	N.D.	87.52 ± 0.36
Protein	0.58 ± 0.08	4.73 ± 0.38	1.43 ± 0.72	2.11 ± 0.42
Total crude fiber	5.16 ± 0.49	5.23 ± 0.62	13.49 ± 0.34	2.43 ± 0.74
Ash	3.68 ± 0.11	3.16 ± 0.13	4.55 ± 0.51	4.64 ± 0.51
Others	3.76 ± 0.27	3.46 ± 0.34	4.26 ± 0.48	2.46 ± 0.24

Results are given in dry bases as Mean ± S.E.; ND – Not Detectable.

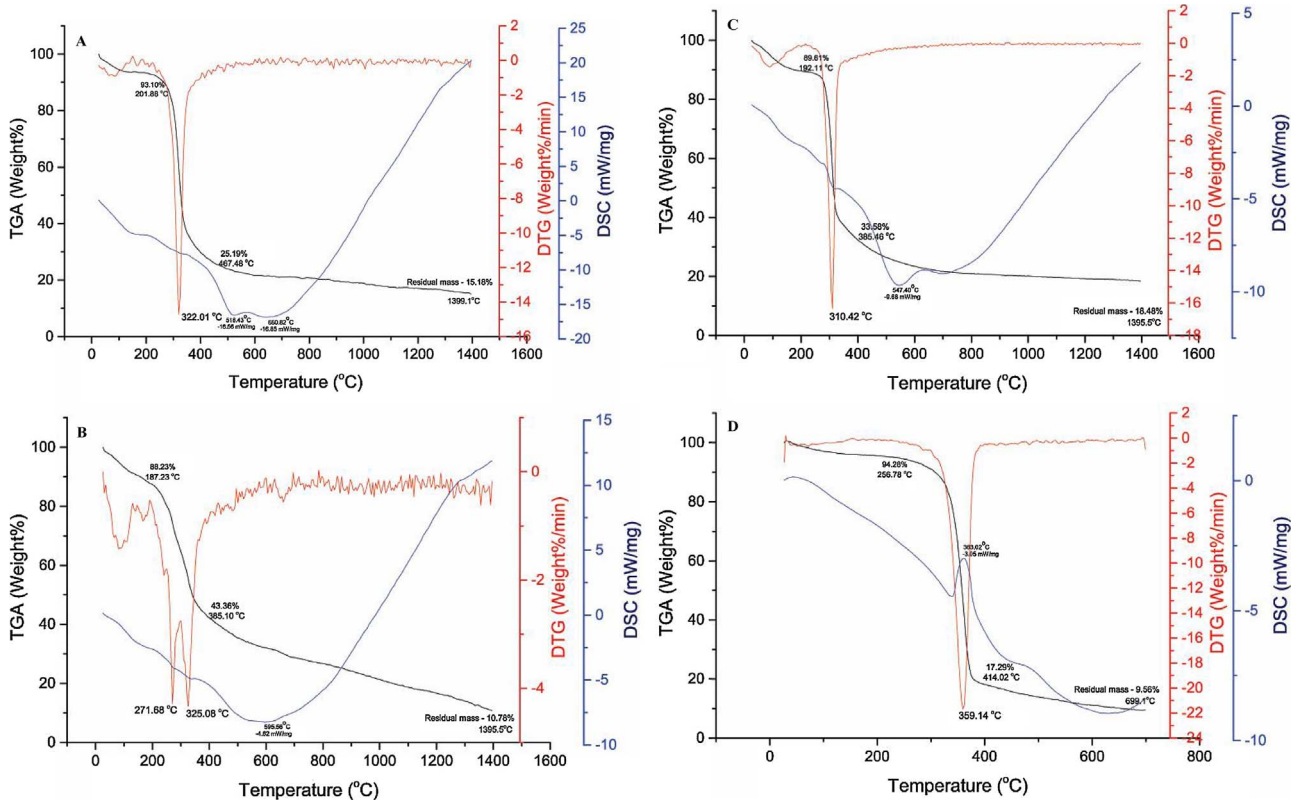

Fig. 1. TG-DSC analysis results of extracted Bio-thermoplastic polysaccharides [Tamarind seed starch [A], Okra mucilage [B], Rice bran starch [C], Sugarcane bagasse cellulose [D]].

found to be 10.78% at 1395.5 °C. Differential scanning calorimetric analysis of okra polysaccharides showed exothermic peak of decomposition at 595.58 °C with energy release of 248.99 mJ/mg. Since the major decomposition of okra polysaccharide starts approximately at 200 °C, similar to other reports (Lousinian, Dimopoulou, Panayiotou, & Ritzoulis, 2017; Prajapati et al., 2013), any process involving okra polysaccharide biopolymer should commence below this temperature to avoid any deformation in products produced using okra waste biopolymer.

Fig. 1C, shows the thermal analysis curves of Residual rice bran starch. Initial weight loss corresponding to moisture loss was observed till 110 °C. Single major weight loss (56.03%) of Residual rice bran starch was observed between 192.11 °C and 385.46 °C, with peak weight loss observed in derivative weight loss curve at 310.42 °C. Similar observation of major weight loss ~300 °C was noted by other researchers (Sudharsan et al., 2016; Puncha-arnon & Uttapap, 2013). Beyond 385.46 °C, there was a constant weight loss in Residual rice bran starch till 1395.5 °C, with residual mass of 18.48%. Differential scanning calorimetric curve of Residual rice bran starch showed two prominent exothermic peaks of decomposition at 547.40 °C and 698.14 °C, with energy release of 172.52 mJ/mg and 82.14 mJ/mg, respectively. Two minor endothermic peaks were also noted at 110.14 °C and 316.25 °C, in which first peak may corresponds to gelatinization of starch and second peak may corresponds to melting of starch (happened during major weight loss period). Gelatinization parameters have been shown to be influenced by the molecular structure (Lee et al., 2017; Noda, Nishiba, Satto, & Soda, 2003). Park, Ibanez, Zhong, and Shoemaker (2007) reported that gelatinization temperatures positively correlated with long chains of amylopectin.

Fig. 1D, shows the thermal analysis curves of sugarcane bagasse cellulose. Based on the TG weight loss curve it can be seen that sugarcane bagasse cellulose had a major weight loss (76.99%) of decomposition between 256.78 °C and 412.02 °C. According to (Kar, 2011; Ding et al., 2013), thermal gravimetric analysis curves of any cellulose material can be divided into three parts; representing loss of water (initial moisture loss), volatization of hemicellulose like contents, and decomposition of cellulose. Peak weight loss temperature was found to be 359.14 °C, confirmed by DTG derivative weight loss curve. According to differential scanning calorimetric analysis, initially SBC was found to absorb heat then it started releasing heat at constant rate (confirmed by exothermic steep at the range of 100–330 °C), till it reaches major weight loss of decomposition. During decomposition at the peak weight loss, prominent endothermic peak was observed at 363.02 °C (45.81 mJ/mg). This endothermic peak may attribute to volatization of hemicellulose, which takes up the heat (Zhang et al., 2016; Hu et al., 2014). Same pattern of thermal decomposition and heat flow was observed in thermal analyses of other cellulose materials (Ccorahua, Troncoso, Rodriguez, Lopez, & Torres, 2017; Gong, Li, Xu, Xiang, & Mo, 2017).

3.1.3. X-ray diffraction and crystallinity index of polysaccharides

Fig. 2, depicts the X-ray diffraction analysis of extracted agro based polysaccharides. Okra mucilage polysaccharides (OMP) showed characteristic peaks at 22.59 and 36.7° (2θ), which may attribute to crystal atomic planes of (111) and (100), respectively (Ghori et al., 2017; Fortunati et al., 2013). Crystallinity index of OMP was estimated to be 28.95%. Fortunati et al. (2013) has proved that crystallinity of OMP can be improved by modification; they have also infused the okra mucilage with poly lactic acid for production of biodegradable stable polymers. X-ray diffractrogram of Residual rice bran starch showed its characteristic peaks at 17.17, 23.28 and 33.28° (2θ), which may attribute to crystal atomic planes of (100), (100) and (110), respectively. Peak pattern of Residual rice bran starch exhibits characteristic peaks of A type starch (Woggum, Sirivongpaisal, & Wittaya, 2015; Cano et al., 2014), with one un-assignable peak at 33.28°. Crystallinity index of RS was estimated to be 28.55%. Some researchers have noted that crystallinity of rice starch can be improved by chemical modification of its amylose structure (Woggum et al., 2015; Colussia et al., 2014).

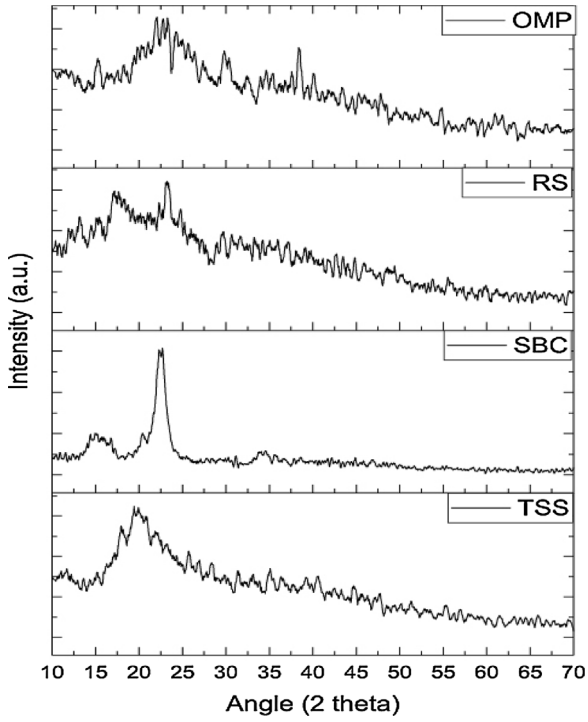

Fig. 2. X-Ray diffractrogram pattern of isolated Bio-thermoplastic polysaccharides.

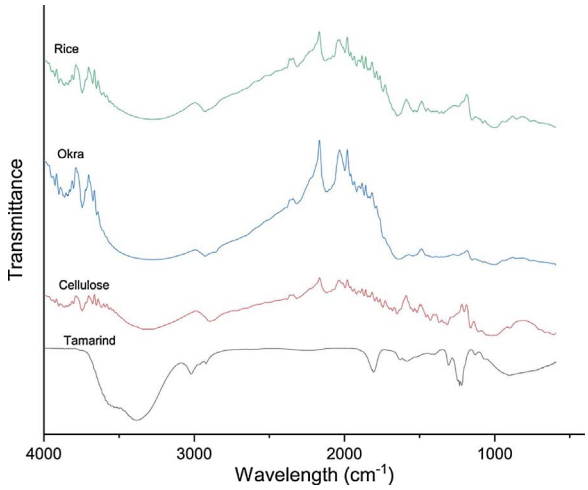

Fig. 3. Fourier transform infrared spectroscopic bands of isolated Bio-thermoplastic polysaccharides.

Sugarcane bagasse cellulose showed its characteristic peaks at 15.13, 20.35, 22.53 and 34.25° (2θ), which may attribute to crystal atomic planes of (110), (100), and (200) and (110), respectively. Similar observations are made by other researchers (Gutierrez & Alvarez, 2017; Gong et al., 2017). Crystallinity index of SBC was estimated to be 73.21%, which was found to be higher than that of balsawood cellulose (62%) and lower than that of corncob (78%) (Liu, Li, Xie, & Deng, 2017; Ditzel, Prestes, Carvalho, Demiate, & Pinheiro, 2017). Tamarind seed starch showed its characteristics XRD peaks at 11.07° (111), 20.09° (110) and 27.43° (210). In this, 11.07 and 20.09° showed the characteristic peaks of A type starch (Lee et al., 2017). Thus, urigam variety of tamarind seed was found to be rich in A type starch, these results are in contrast with our previous study on DTS-1 variety of tamarind seeds (Sudharsan et al., 2016). Crystallinity index of TSS was found to be 31.07%.

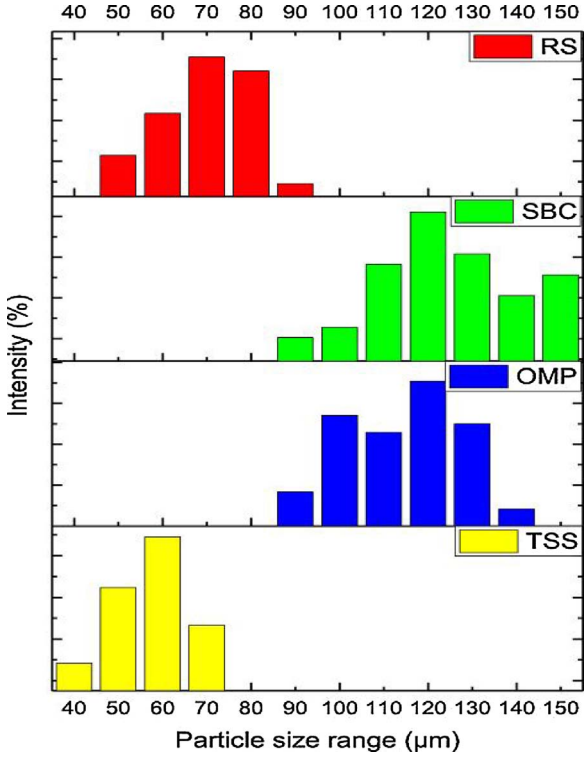

Fig. 4. Particle size distribution of Bio-thermoplastic polysaccharides extracted from agro industrial wastes.

3.1.4. Characterization of functional groups present in polysaccharides

Fourier transform infrared bands of isolated polysaccharides were depicted in Fig. 3. IR spectral band pattern of Residual rice bran starch showed intense peak at 3272 cm^{-1} (corresponding to hydroxyl group, polymeric O—H stretch) (Colussia et al., 2014). Associated intense peak at 2933 cm^{-1} (C—H Asym./Sym. Stretch) confirms the presence of $-CH_2$ group (Woggum et al., 2015). Bands at 2302 and 2113 cm^{-1} shows the presence of characteristic alkyne group. Intense peak at 1640 cm^{-1} corresponding to N—H bend of primary amines, shows that Residual rice bran starch still contains some protein molecules even after alkaline extraction (Sudharsan et al., 2016). Minor peaks at 1516, 1149 and 1001 cm^{-1} indicates the C—H skeletal vibrations (Colussia et al., 2014).

IR spectral pattern of OMP showed intense polymeric O—H stretch peak at 3325 cm^{-1} (Archana et al., 2013). Associated band at 2929 cm^{-1} indicates the presence of $-CH_2$ group (Fortunati et al., 2013). Bands at 2313 and 2113 cm^{-1}, shows the presence of characteristic alkyne group. Intense band at 1998 cm^{-1} (C—N bond stretch), confirms the binding of proteins with mucilage of okra (Alamri et al., 2017). Band at 1645 cm^{-1} corresponds to N—H primary amine bend also confirms the presence of associated proteins with OMP (Alamri et al., 2017; Archana et al., 2013). Minor peak at 1154 cm^{-1}, shows the C—H skeletal vibrations.

IR spectral pattern of SB cellulose was found to have intense broad polymeric O—H stretch band at 3315 cm^{-1} (Liu et al., 2017). Band at 2895 cm^{-1} associated with O—H stretch corresponds to C—H stretching vibrations. Minor band at 2118 cm^{-1}, represent the characteristic alkyne group. Minor peaks at 1655 and 1521 cm^{-1} corresponds to secondary amine and Asymmetric N—H bends, respectively. 1159 cm^{-1} spectral band may correspond to C—H skeletal vibration (Wang, Yao, Zhou, & Zhang, 2017). Other minor bands at 1025 and 891 cm^{-1}, indicated the primary amine N—H stretch and COC stretching at 1–4 glycosidic linkage in SB cellulose (Liu et al., 2017), respectively.

Tamarind seed starch IR spectral band pattern showed characteristic broad O—H polymeric stretch at 3387 cm^{-1}. Minor band at 3014 cm^{-1}

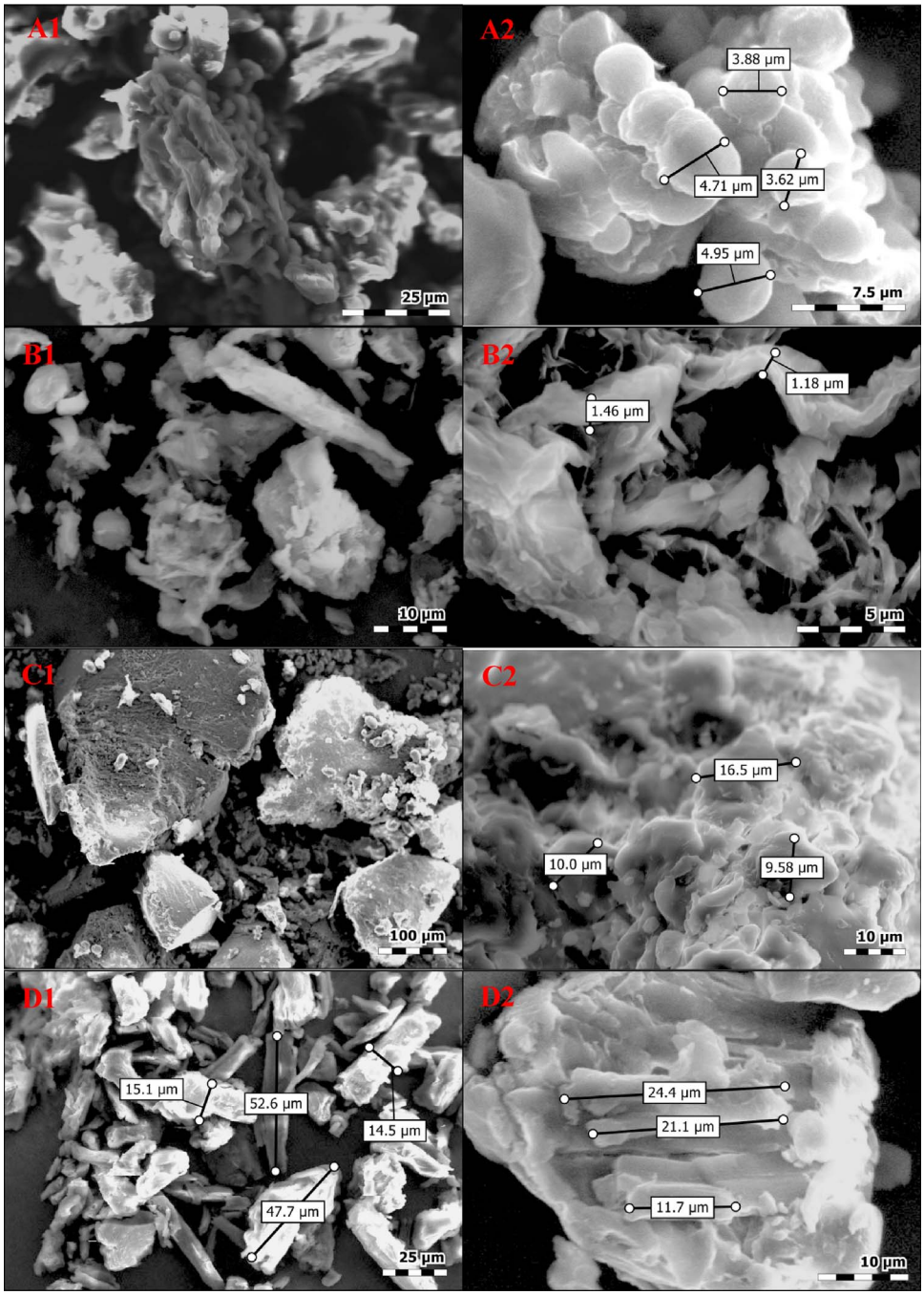

Fig. 5. Surface morphology of extracted polysaccharides [Tamarind seed starch [A], Okra mucilage [B], Rice bran starch [C], Sugarcane bagasse cellulose [D]].

correspond to overlap of C—H and O—H stretches was also noted [Samal & Dangi, 2014]. Peaks at 2910 and 1807 cm^{-1}, indicated the C—H stretching vibration and carboxyl stretching vibrations, respectively. Minor peaks at 1578, 1221 and 1130 cm^{-1}, may correspond to C—H skeletal vibrations. Peaks at 1302 and 891 cm^{-1} were noted to indicate the C—H bend of aliphatic CH_2 and COC stretching of glycosidic linkages in tamarind seed starch (Sudharsan et al., 2016), respectively. From the IR spectral analysis of TSS it is evident, that employed multistage alkali wash of TSS, completely removed the protein molecules present in tamarind seed powder (confirmed by absence of characteristic bands corresponding to primary and secondary amine).

3.1.5. Particle size analysis and morphology of polysaccharides

Particle size distribution of extracted Bio-thermoplastic polysaccharides was depicted in Fig. 4. Residual rice bran starch was found to be having starch globules in size range between 50 and 90 µm. 70–80 µm was found to be the major particle size distribution with high intensities of laser particle analysis. Dhital et al. (2015) investigated different rice verities for its particle size and reported the size distribution of rice starch granules to be between 10 and 1000 µm, depending on the verity. Average particle size of RS starch was found to be 70 µm. Particle size of native cellulose can be ranged between 50 and 500 µm (Wang et al., 2017). These cellulose molecules can be treated with chemical or physical means to convert them to Nano crystalline cellulose molecules (Liu et al., 2017). Sugarcane bagasse cellulose was found to have cellulose molecules at the broad size range between 90 and 150 µm. 120 µm size ranged particles were examined to be the major and average size particles present in SBC. Okra mucilage polysaccharides were also found to have broad size range distribution between 90 and 140 µm, with major particles at size range of 120 µm.

Lousinian et al. (2017) also reported the particle size range of okra to be between 159 and 68 μm, they have also reported that okra mucilage can exhibit different particle size's at different solvents, depending on the interaction between the side chains of mucilage and corresponding solvent. Average particle size of OMP was estimated to be 115 nm. Sudharsan et al., 2016 has reported the particle size of DTS – 1 variety of tamarind seed starch as between 30 and 130 μm, at which high amount of starch molecules were found to be between 60 and 90 μm. Size distribution of urigam variety tamarind seed starch was found to be in range between 40 and 70 μm, with major particles at size range of 60 μm. Average particle size of TSS was estimated to be 55 μm.

Scanning electron micrographs of polysaccharides extracted from different agro wastes are given in Fig. 5. Surface morphology of tamarind seed starch was depicted in Fig. 5A (1 & 2). Tamarind seed xyloglucan starch molecules were examined to be in the form of globule clusters. Individual starch globules were found to be in the size range of 3.5–5 μm. These starch molecules club together to form clusters of starch globules, which was noted to be in the range of 40–70 μm in particle size analysis. Surface morphology of okra mucilage polysaccharides were depicted in Fig. 5B (1 & 2). Okra mucilage polysaccharide molecules were found to be in the form of irregular linear sheets, similar observations were noted by other researchers (Mishra & Pal, 2007; Dimopoulou, Ritzoulis, Papastergiadis, & Panayiotou, 2014). Each sheet of okra mucilage was noted to be having width size of 1–2 μm, but its length may be at the range of 90–140 μm, as given in particle size analysis. The biosynthesis of starch occurs in amyloplasts. Rice grain amyloplasts contain several starch granules (granula) tightly packed as apparently compound granules. Such granules are often rounded at first, but become angular as they pack together within the amyloplast (Dhital et al., 2015). Surface morphology of Residual rice bran starch molecules were depicted in Fig. 5C (1 & 2). Residual rice bran starch was found to be irregularly shaped starch granules associated with proteins and fibers. Each rice starch granules were measured to be in the size range of 9–20 μm, with their clusters having average particle size of 70 μm. These granules do not separate during starch extraction because they are fused together by a surrounding layer of apparently amorphous starch (Wei et al., 2010; Gott, Barton, Samuel, & Torrence, 2006). Surface morphology of sugarcane bagasse cellulose molecules were depicted in Fig. 5D (1 & 2). Sugarcane bagasse cellulose molecules were to be in shape of linear bundles, due to cohesive nature of cellulose fibers (Wang et al., 2017). Each bundle seems to be in the width size range of 10–15 μm and length size range of 20–50 μm from SEM images.

4. Conclusions

All the investigated natural biopolymers were found to be having high thermal stability, in the order of SBC > TSS > RS > OMP. Okra mucilage polysaccharide was found to having low thermal degradation properties. Thus, thermally stable SBC, TSS and RS can be utilized as a matrix for development of Bio-thermoplastics. Crystallinity index of investigated polysaccharides were in order of SBC > TSS > RS > OMP, which correlates with the thermal stability analysis. This result indicates that amount of crystalline molecules present in polysaccharides directly proportional to thermal stability of polysaccharides. Sugarcane bagasse cellulose was estimated to be having very high crystallinity index of 73%.

Acknowledgements

The authors sincerely express their greatest gratitude to DST, Science and Engineering Research Board (SERB/MOFPI/0022/2014) for financial support. First author would like to express his sincere thanks to Council of scientific and industrial research – CSIR for award of senior research fellowship (No. 09/468/0500/2016/EMR-I).

References

AOAC Official Method 996.11 (1996). Starch (total) in cereal products: Amyloglucosidase–amylase method. In W. Horwitz (Ed.). *Official methods of analysis of AOAC International*. Gaithersburg, Maryland, United States: AOAC International.
AOCS Official Method Ba 4a-38 (1997a). Nitrogen-ammonia-protein modified Kjedahl method. In D. Firestone (Ed.). *Official methods and recommended practices of the AOCS*. Champaign, IL, USA: American Oil Chemists' Society.
AOCS Official Method Ba 5a-49 (1997b). Ash. In D. Firestone (Ed.). *Official methods and recommended practices of the AOCS*. Champaign, IL, USA: American Oil Chemists' Society.
Alamri, M. S., Mohamed, A., Hussain, S., & Xu, J. (2017). Effect of okra extract on properties of wheat, corn and rice starches. *Journal of Food Agriculture & Environment, 10*(1), 217–222.
Archana, G., Sabina, K., Babuskin, S., Radhakrishnan, K., Fayidh, M. A., Saravana, A., et al. (2013). Preparation and characterization of mucilage polysaccharide for biomedical applications. *Carbohydrate Polymers, 98*, 89–94.
Candido, R. G., & Gonclave, A. R. (2016). Synthesis of cellulose acetate and carboxymethyl cellulose from sugarcane straw. *Carbohydrate Polymers, 152*, 679–686.
Cano, A., Jimenez, A., Chafer, M., Gonzalez, C., & Chiralt, A. (2014). Effect of amylose: Amylopectin ratio and rice bran addition on starch films properties. *Carbohydrate Polymers, 111*, 543–555.
Ccorahua, R., Troncoso, O. P., Rodriguez, S., Lopez, D., & Torres, F. G. (2017). Hydrazine treatment improves conductivity of bacterialcellulose/graphene nanocomposites obtained by a novel processing method. *Carbohydrate Polymers, 171*, 68–76.
Chandra mohan, C., Rakhavan, K. R., Sudharsan, K., Radha Krishnan, K., Babuskin, S., & Sukumar, M. (2016). Design and characterization of spice fused tamarind starch edible packaging films. *LWT-Food Science and Technology, 68*, 642–652.
Colussia, R., Pintoa, V. Z., Halal, S. L. M. E., Vaniera, N. L., Villanova, F. A., Marques e Silva, R., et al. (2014). Structural, morphological, and physicochemical properties of acetylated high-, medium-, and low-amylose rice starches. *Carbohydrate Polymers, 103*, 405–413.
Dhital, S., Butardo, V. M., Jr., Jobling, S. A., & Gidley, M. J. (2015). Rice starch granule amylolysis –Differentiating effects of particle size, morphology, thermal properties and crystalline polymorph. *Carbohydrate Polymers, 115*, 305–316.
Dimopoulou, M., Ritzoulis, C., Papastergiadis, E. S., & Panayiotou, C. (2014). Composite materials based on okra hydrocolloids and hydroxyapatite. *Food Hydrocolloids, 42*, 348–354.
Ding, D., Zhao, Y., Yang, S., Shi, W., Zhang, Z., Lei, Z., et al. (2013). Adsorption of cesium from aqueous solution using agricultural residue e Walnut shell: Equilibrium, kinetic and thermodynamic modeling studies. *Water Research, 47*, 2563–2571.
Ditzel, F. I., Prestes, E., Carvalho, B. M., Demiate, I. M., & Pinheiro, L. A. (2017). Nanocrystalline cellulose extracted from pine wood and corncob. *Carbohydrate Polymers, 157*, 1577–1585.
Dos Santos, T. P., Leonel, M., Garcia, E. L., do Carmo, E. L., & Franco, C. M. (2016). Crystallinity, thermal and pasting properties of starches from different potato cultivars grown in Brazil. *International Journal of Biological Macromolecules, 82*, 144–149.
Fortunati, E., Puglia, D., Monti, M., Santulli, C., Maniruzzaman, M., Foresti, M. L., et al. (2013). Okra (Abelmoschus esculentus) fibre based PLA composites: Mechanical behaviour and biodegradation. *Journal of Polymers and the Environment, 21*(3), 726–737.
Ghori, M. U., Mohammad, M. A., Rudrangi, S. R. S., Fleming, L. T., Merchant, H. A., Smith, A. M., et al. (2017). Impact of purification on physicochemical, surface and functional properties of okra biopolymer. *Food Hydrocolloids, 71*, 311–320.
Gong, J., Li, J., Xu, J., Xiang, Z., & Mo, L. (2017). Research on cellulose nanocrystals produced from cellulose sources with various polymorphs. *RSC Advances, 7*, 33486–33493.
Gott, B., Barton, H., Samuel, D., & Torrence, R. (2006). Biology of starch. In R. Torrence, & H. Barton (Eds.). *Ancient starch research* (pp. 35–45). Walnut Creek, CA, USA: Left Coast Press.
Goyal, P., Kumar, V., & Sharma, P. (2007). Carboxymethylation of Tamarind kernel powder. *Carbohydrate Polymers, 69*, 251–255.
Gutierrez, T. J., & Alvarez, V. A. (2017). Cellulosic materials as natural fillers in starch-containing matrix-based films: A review. *Polymer Bulletin, 74*(6), 2401–2430.
Hu, Y., Tang, L. R., Lu, Q. L., Wang, S. Q., Chen, X. R., & Huang, B. (2014). Preparation of cellulose nanocrystals and carboxylated cellulose nanocrystals from borer powder of bamboo. *Cellulose, 21*(3), 1611–1618.
Imam, S. H., Chiou, B. S., Woods, D., Shey, J., Glenn, G. M., Orts, W. J., et al. (2008). Starch/pulp-fiber based packaging foams and cast films containing Alaskan fish by-products (waste). *BioResources, 3*(3), 758–773.
Kar, Y. (2011). Co-pyrolysis of walnut shell and tar sand in a fixedbed reactor. *Bioresource Technology, 102*(20), 9800–9805.
Kasa, S. N., Omar, M. F., Abdullah, M. M. A. B., Ismail, I. N., Ting, S. S., Vac, S. C., et al. (2017). Effect of unmodified and modified nanocrystalline cellulose reinforced polylactic acid (PLA) polymer prepared by solvent casting method. *Material Plastic, 54*(1), 91–97.
Lee, S., Lee, J. H., & Chung, H. J. (2017). Impact of diverse cultivars on molecular and crystalline structures of rice starch for food processing. *Carbohydrate Polymers, 169*, 33–40.
Liu, Z., Li, X., Xie, W., & Deng, H. (2017). Extraction, isolation and characterization of nanocrystalline cellulosefrom industrial kelp (Laminaria japonica) waste. *Carbohydrate Polymers, 173*, 353–359.
Lousinian, S., Dimopoulou, M., Panayiotou, C., & Ritzoulis, C. (2017). Self-assembly of a food hydrocolloid: The case of okra mucilage. *Food Hydrocolloids, 66*, 190–198.
Mishra, A., & Pal, S. (2007). Polyacrylonitrile-grafted Okra mucilage: A renewable

reservoir to polymeric materials. *Carbohydrate Polymers, 68*, 95–100.
Mishra, A., & Sunita, P. (2007). Polyacrylonitrile-grafted okra mucilage: A renewable reservoir to polymeric materials. *Carbohydrate Polymers, 68*, 95–100.
Noda, T., Nishiba, Y., Satto, T., & Soda, I. (2003). Properties of starches from several low-amylose rice cultivars. *Cereal Chemistry, 80*, 193–197.
Park, I. M., Ibanez, A. M., Zhong, F., & Shoemaker, C. F. (2007). Gelatinization and pasting properties of waxy and non-waxy rice starches. *Starch, 59*, 388–396.
Prajapati, V. D., Jani, G. K., Moradiya, N. G., & Randeria, N. P. (2013). Pharmaceutical applications of various natural gums, mucilages and their modified forms. *Carbohydrate Polymers, 92*, 1685–1699.
Prosky, L., Asp, N. G., Scheweizer, T. F., de Vries, J. W., & Furda, I. (1988). Determination of insoluble, soluble and total dietary fiber in foods and food products: Interlaboratory study. *Journal −Association of Official Anaytical Chemists, 71*(5), 1017–1023.
Puncha-arnon, S., & Uttapap, D. (2013). Rice starch vs. rice flour: Differences in their properties when modified by heat–moisture treatment. *Carbohydrate Polymers, 91*, 85–91.
Sadasivam, S., & Manickam, A. (1996). *Biochemical methods.* New Delhi, India: New Age International.
Samal, P. K., & Dangi, J. S. (2014). Isolation, preliminary characterization and hepato-protective activityof polysaccharides from Tamarindus indica L. *Carbohydrate Polymers, 102*, 1–7.
Sengkhamparn, N., Verhoef, R., Schols, H. A., & Sajjaanantakul, T. (2008). Characterization of cell wall polysaccharides of okra. *Carbohydrates Research, 344*, 1824–1832.
Sudharsan, K., Chandra Mohan, C., Azhagu Saravana Babu, P., Archana, G., Sabina, K., Sivarajan, M., et al. (2016). Production and characterization of cellulose reinforced starch (CRT) films. *International Journal of Biological Macromolecules, 83*, 385–395.
Updegraff, D. M. (1969). Semimicro determination of cellulose inbiological materials. *Analytical Biochemistry, 32*(3), 420–424.
Wang, H. J., Sun, C., & Huang, L. Q. (2010). Preparation and properties of whey protein packaging film. *Proceedings of the 17th IAPRI world conference on packaging* (pp. 259–264).
Wang, Z., Yao, Z. J., Zhou, J., & Zhang, Y. (2017). Reuse of waste cotton cloth for the extraction of cellulose nanocrystals. *Carbohydrate Polymers, 157*, 945–952.
Wei, C., Qin, F., Zhu, L., Zhou, W., Chen, Y., Wang, Y., et al. (2010). Microstructure and ultrastructure of high-amylose rice resistant starch granules modified by antisense RNA inhibition of starch branching enzyme. *Journal of Agricultural and Food Chemistry, 58*(2), 1224–1232.
Woggum, T., Sirivongpaisal, P., & Wittaya, T. (2015). Characteristics and properties of hydroxypropylated rice starch based biodegradable films. *Food Hydrocolloids, 50*, 54–64.
Yuliana, M., Huynh, L. K., Hob, Q. P., Truong, C. T., & Ju, Y. H. (2012). Defatted cashew nut shell starch as renewable polymeric material: Isolation and characterization. *Carbohydrate Polymers, 87*, 2576–2581.
Zhang, K., Suna, P., Liua, H., Shang, S., Song, J., & Wang, D. (2016). Extraction and comparison of carboxylated cellulose nanocrystals from bleached sugarcane bagasse pulp using two different oxidation methods. *Carbohydrate Polymers, 138*, 237–243.